Chapter 1

INTRODUCTION

Supercapacitors are energy storage systems that have better power density, excellent reversibility and longer cycle life than batteries, and have higher energy density as compared with conventional capacitors [1]. They have tremendous applications in many fields which include power sources for vehicles, backup-power systems, and supplementary power of fuel and energy cells to limit the power constraints [1-4]. This increasing energy and power demands have stimulated the research on the development of new electrode materials for supercapacitors. The nanostructured materials with high surface area and surface porosity are considered to be the most promising electrode materials for supercapacitor devices.

Manganese dioxide (MnO_2) as the cathode material for supercapacitors has been widely investigated because of its low-cost, abundance, non-toxicity and high theoretical specific capacitance of 1370 F/g [5–7]. However, its practical specific capacitance is low compared with the high-cost RuO_2. It is believed that the low energy density of MnO_2 is caused by its charge storage mechanism and poor electrical conductivity, which is based on ion adsorption or redox reactions on the surface layer [8, 9]. In a typical charge–discharge process, only the first few nanometers from the surface can be utilized, resulting in low utilization and limited energy densities [10-15] Therefore, improving the utilization of active material is the key to enhance energy and power density of the electrode material.

Research objectives

The foremost aim of this research work is to synthesis some highly performing and cost effective cathode materials based on α-MnO_2. The main focus of the research study includes:

1. Identification of cost effective fabrication techniques to synthesis MnO_2 nanostuctures.
2. Fabrication of highly porous and stable electrode using nanostructured MnO_2.
3. Characterization of these electrode using different characterization techniques which includes cyclic voltammetry, charge discharge studies, electrochemical impedance spectroscopy etc.
4. Fabrication and testing of fully functional supercapacitor device.

Chapter 2

MATERIALS AND METHODS

2.1. Nano-wire preparation

The chemicals used in the present study were of analytical grade obtained from Sigma Aldrich. 0.1M $MnSO_4$ and 0.1M $KMnO_4$ were dissolved in 30 mL distilled water. To this 1mL of H_2SO_4 (60 % concentration) was added under vigorous stirring conditions for 30 mins. The prepared solution was transferred to a 100 mL Teflon-coated container and autoclaved at 150 ˚C for different time intervals ranging from 30 mins-36 h. The resultant solution was centrifuged for 30 mins and the obtained precipitate was thoroughly washed using distilled water and dried at 60 ˚C for 4 h.

2.2. Preparation of spongy composite electrode using freeze drying method

All the chemicals used in the present study were of analytical grade. 5 wt% PVA solution was mixed with polyethylene dioxythiophene- polystyrene sulphonate (PEDOT-PSS) (Alfa Aesar, India) for 30 min. Different amounts of MnO_2 (5, 10 and 20 wt%) powder (Nice Chemicals, India, particle size ~50 nm) were added to the above mixture and stirred overnight. This stirred solution was aged at 20 ^{0}C for 24 hrs and then freeze dried (lyophilized) using a lyophilizer (ALPHA 2-4 LD plus) for 24 hrs. Depending on the amount of MnO_2 embedded into the PEDOT: PSS as matrix material, these spongy samples were designated as PPM-5, PPM-10 and PPM-20, where PP and M denotes PEDOT: PSS and MnO_2 respectively. The number represents the amount of wt % of MnO_2 added to the PEDOT: PSS matrix.

2.3. Preparation of carbonized MnO_2 nano-wires

The synthesis of MnO_2 nanowires used in the present study is similar to the procedure as discussed in the second chapter. To describe briefly, 0.1M $MnSO_4$ (Sigma Aldrich) and 0.1M $KMnO_4$ (Sigma Aldrich) were separately dissolved in 30 mL distilled water. To this solution 1 mL of H_2SO_4 (Sigma Aldrich) (60 % concentration) was added under vigorous stirring conditions. This solution mixture was transferred to a teflon-coated container and autoclaved at 150°C for 24 h. The resultant solution was centrifuged and the obtained precipitates were thoroughly washed using distilled water and dried in air at 40 ºC. These MnO_2 nanowires were carbonized with carbon nano-beads through pyrolsis of camphor blocks (Jyothi Chemicals, India).

2.4. Electrophoretic deposition and surface characterization

Morphology and phase analysis were performed using transmission electron microscopy-selective area energy dispersive X-ray (TEM, Model: JEOL, JEM-2100F) and X-ray diffraction analysis (XRD, X'Pert PRO Analytical), respectively. Image J software was used to determine the diameter size distribution of the nanowires. The resultant nanowires were electrophoretically deposited onto a titanium substrate. For this an electrochemical setup comprising of titanium foil (1cm × 1cm × 0.2 mm) was used as substrate (cathode) and platinum wire as an anode. Isopropanol solution was used as the electrolytic solvent. To this electrolyte, 5 mg of nanopowder were dispersed uniformly under constant stirring. The deposition was carried out at 40 V for 30 mins at room temperature, resulting in a thin uniform porous electrode. The surface porosity was determined by quantitative image analysis (using GMDH software, Charlottesville, VA) from the SEM images. Atomic force microscopy (AFM) (JEOL SPM 5200) and Profilometer (Veeco Dektak 150) were used to measure the surface roughness and thickness of the deposited layer. Surface area measurements were obtained using BET analyzer (Nova Quantachrome, USA).

2.5. Electrochemical characterization

Cyclic voltammetry (CV) and constant current charge-discharge were performed to evaluate the capacitance. Electrochemical impedance spectroscopy (EIS) (electrochemical workstation: Newport Model) was performed under a biased potential of 0.2V to measure the charge transfer resistance of the prepared electrode. For the above electrochemical studies, a three electrode setup consisting of MnO_2 based electrode, platinum and calomel electrode were used as working, counter and reference electrode respectively.

Chapter 3

RESULTS AND DISCUSSIONS

3.1. Morphological effect on cycling stability and overall performance of MnO_2 based supercapacitor

3.1.1. Phase and morphological analysis of MnO_2 nanowire

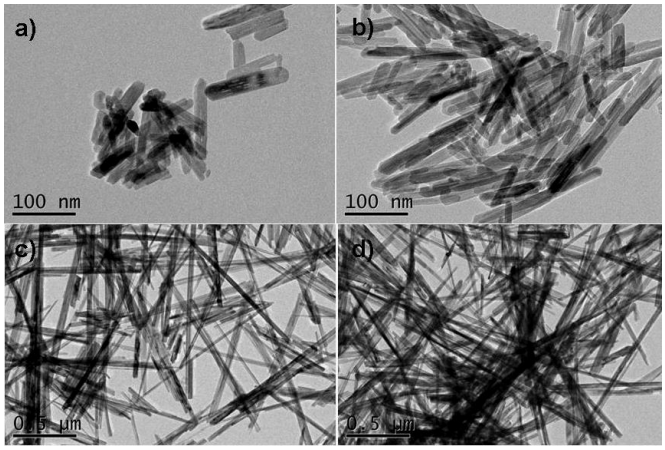

Fig.3.1.TEM images displaying the morphology of α-MnO_2 synthesized hydrothermally at different times of a) 30 min b) 1h c) 24 h and d) 36 h.

Fig. 3.1. (a-d) shows the TEM images displaying the morphology of hydrothermally synthesized MnO_2 at different processing times of 30 mins, 1h, 24 h and 36 h. It was observed that, as the processing time increases from 30 mins to 36 h the morphology changes from nanorods to nanowires. Fig. 3.2 shows the XRD pattern of the synthesized nanowires where the diffraction peaks corresponded to pure tetragonal phases of α-MnO_2 (JCPDS 44-0141).

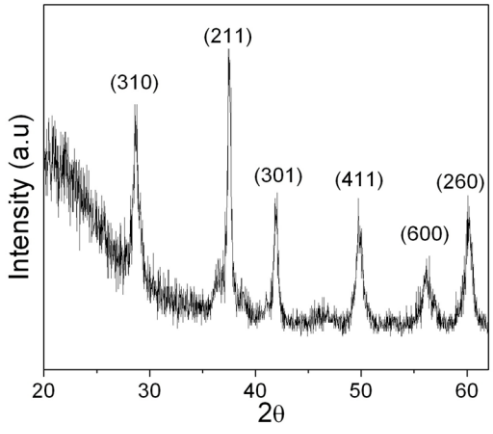

Fig. 3.2. XRD pattern of the synthesized nanowires.

Fig. 3.3(a) shows the wire diameter size analysis for these nanowires, which showed a narrow skewed distribution. The diameter was found to be in the range of 5-40 nm centered at ~20 nm. Fig. 3.3(b) reveals the SEM image of eletrophoretically deposited layer of α-MnO_2 nanowires. It was observed that these wires were randomly oriented and exhibited a highly porous network-like structure. Fig. 3.3(c&d) shows the cross-sectional SEM and AFM image of the MnO_2 nanowire on Ti foil showing a coating thickness of ~20 µm.

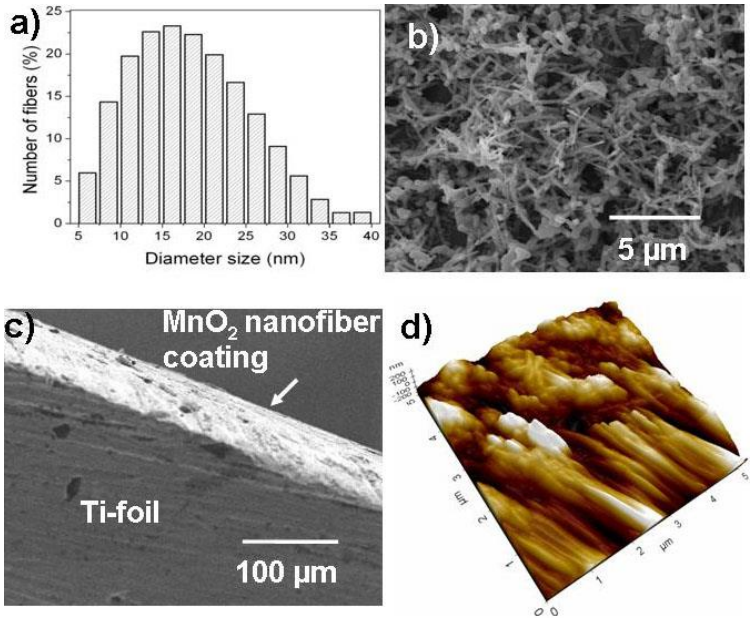

Fig.3.3. a) The wire diameter size analysis and b) SEM image of eletrophoretically deposited layer of α-MnO_2 nanowires c) cross-sectional and d) AFM image of α-MnO_2 nanowires layer.

3.1.2. Electrochemical characterization

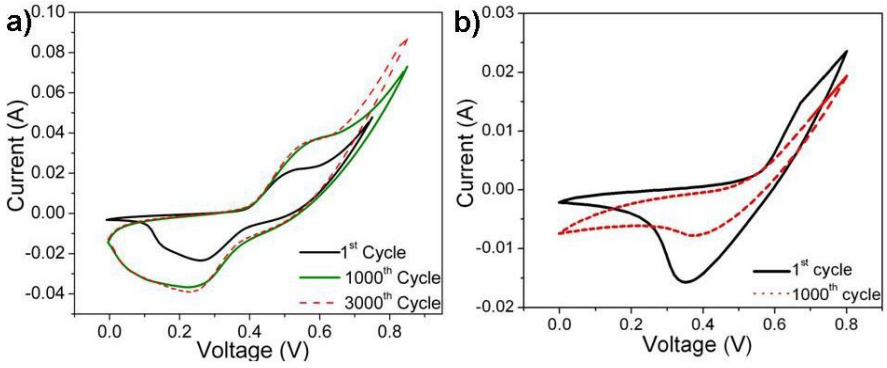

Fig.3.5. CV curves recorded for a) nanowire MnO_2 at 1st and 3000th cycle b) nanoparticulate MnO_2 at 1st and 1000th cycle showing 27 % fading.

For further understanding on the role of surface area, nanowire-based electrodes were compared with electrodes prepared using a commercially available MnO_2 powder (Nice Chemicals, India, particle size: ~ 50-80 nm). Capacitance fading was observed in nanoparticulate electrode at the end of 1000th cycle (Fig. 3.5b).

3.2. Sythesis and characterization of MnO_2/PEDOT:PSS composite cathodes

3.2.1. Morphological analysis of MnO_2 / PEDOT: PSS

Fig. 3.6 shows the SEM image of PPM-10 (90wt% PEDOT: PSS/ 10Wt% MnO_2) samples under lyophilized condition. It was observed that the PPM samples exhibited interconnected macro-pores with sizes ranging from 100-150 μm (Fig. 3.6 (a—c)). SEM images (Fig.3.6 (d—f)) of these PPM-10 scaffolds at higher magnifications revealed a highly roughened surface exhibiting mesoporous structure.

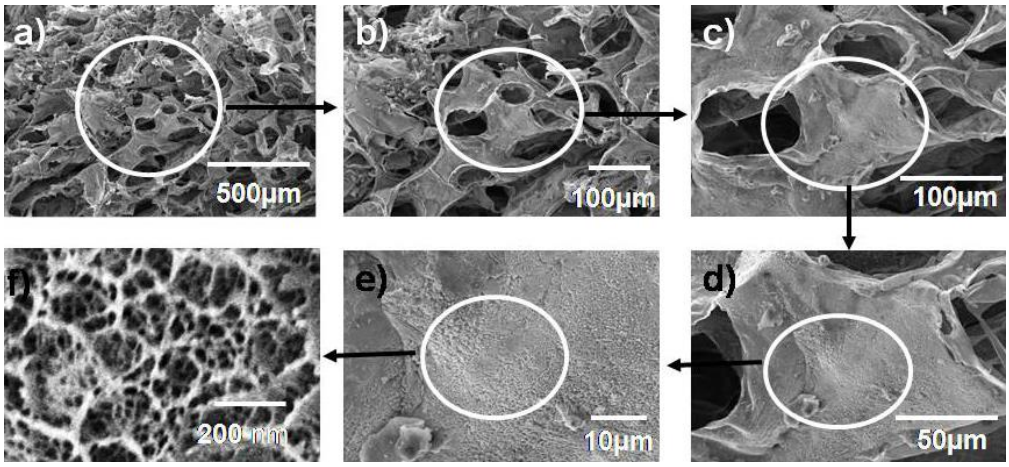

Fig. 3.6.SEM image showing the hierarchical mesoporous structure in PPM-10 hybrid sponges.

3.2.2. Cycling and constant current discharge behavior of ppm-10 electrode

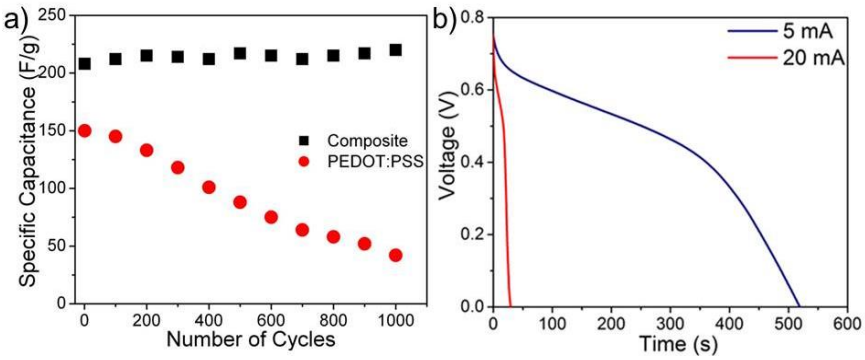

Fig.3.7. a) Cycling stability studies of PPM-10 and PP samples at 100 mV s^{-1} and b) discharge profile of PPM-10 electrode at different discharging currents.

The cycling stability was determined using CV tests for PPM-10 electrodes for 3000 cycles at a scan rate of 100 mV s^{-1} (see Fig.3.7). capacitance fading (20%) was observed at the end of 3000th cycle (Fig.3.7). The maximum energy density of ~78 Wh kg^{-1} at 5 mA and power density of ~6 kW kg^{-1} were achieved for these electrodes.

3.3. Effect of nanocarbon as conducting secondary phase on the overall performance of MnO_2 based supercapacitors

3.3.1. Phase and morphological analysis of nanocarbon

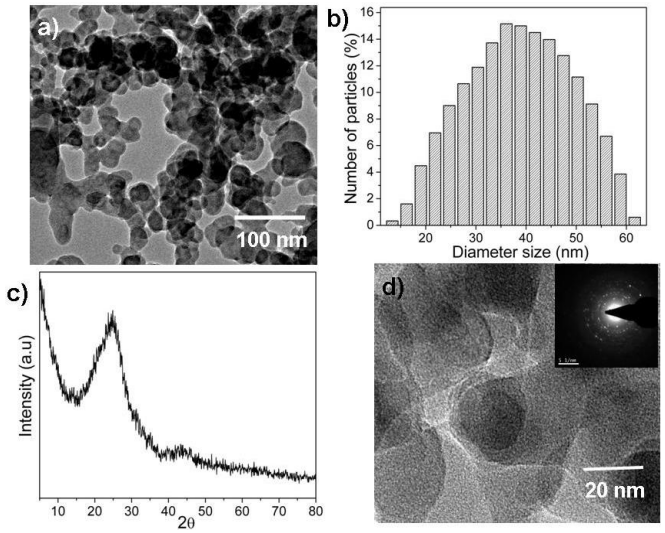

Fig.3.8. a) TEM, b) diameter size distribution, c) XRD and d) HR-TEM (inset- SAED) of camphoric carbon nano-beads.

Fig.3.8.a represents the morphology of camphoric carbon nano-beads obtained via pyrolsis. These nano-beads exhibited a spheroid morphology having particle size distribution varying from 5—70 nm (Fig.3.8b). Fig.3.8c elucidates the phase analysis of these nano-beads, examined by XRD. HR-TEM image is shown in Fig. 3.8d.

3.2.2. Electrochemical characterization of MnO_2 nanowire/nanocarbon systems

In order to determine the optimal electrode composition and apt electrolyte, cyclic voltammetry (CV) tests at a scan rate of 10 mVs^{-1} were performed in LiOH, NaOH and KOH electrolyte (Fig.3.9 (a-d)). The working electrodes comprised of electrophoretically deposited thin films of MC-5, MC-10, MC-20 and MC-50.

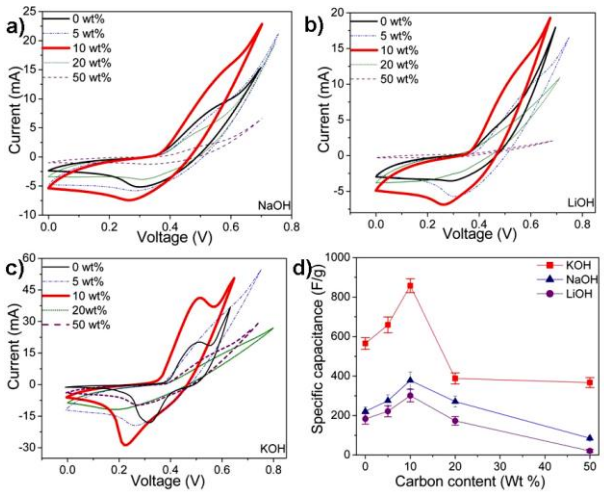

Fig.3. 9. CV curves of MC electrodes with different carbon content in a) NaOH, b) LiOH and c) KOH electrolytes and d) plot showing the variation of specific capacitance with carbon content.

For a given electrode composition, it was observed that the redox peaks were prominent in KOH as compared to LiOH and NaOH electrolytes (Fig.3.9 (a-d)).

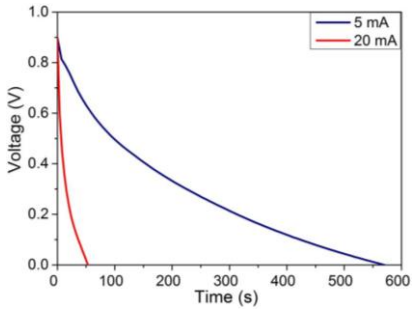

Fig.3.10. discharge curves of MC-10 electrode.

Fig.3.10 displays the constant current discharge performance of MC-10 at different discharging currents. The obtained energy and power density values for these MC-10 electrode were found to be 110 Wh kg^{-1} and 32 kW kg^{-1}, respectively. The energy and power density values for MC-10 were found to be 3 and 5 times higher, respectively than pristine MnO_2 nanowire (Fig.3.10b) and MnO_2/PEDOT:PSS electrodes.

Chapter 4

CONCLUSIONS

The present investigation was mainly concentrated on MnO_2 based electrodes for supercapacitor applications. In the first part MnO_2 nanowire and nanoparticle powders were synthesized by a simple hydrothermal technique. SEM image revealed the presence of these nanostructures. The size of the nanowires was analyzed by TEM image and diameter size distribution curve and it was observed to be ~17nm. SEM images of electrophoretically deposited MnO_2 nanowire electrode showed highly porous in nature as compared to the particulate electrode. The electrochemical performance of both nanowire and nanoparticulate electrodes were carried out. The specific capacitance of MnO_2 nanowire and nanopaticle was found to be 1050 F g^{-1} and 513 F g^{-1}. The energy, power density values of nanoparticulte and nanowire electrode were found out using charge discharge studies and it was found to be 31 Wh/Kg, 4 KW/Kg and 71 Wh/Kg, 6 KW/Kg respectively. This nanowire morphology showed advantages especially from the point of high cycling stability, energy and power densities as compared to the nanoparticle counterpart.

In the second part MnO_2/ PEDOT: PSS composite was fabricated using freeze drying technique. The main intension of this second part is that to improve the conductivity of MnO_2 electrode hence to improve the overall performance of the system. The SEM images of theMnO_2/ PEDOT: PSS system showed hierarchical meso/micro porous structures. This hybrid porous morphology shows advantages especially from points of better surface area and mass specific capacitance. The mean mass specific capacitance value was found to be 1068 F g^{-1} from CV studies. These electrodes exhibited energy and power density values of 78Wh kg^{-1} and 6 kW kg^{-1} respectively.

In the last section MnO_2 / nanocarbon composite was fabricated by using simple pyrolysis technique. Morphological analysis was carried out using SEM and TEM. It was observed that the inclusion of nanocarbon by pyrolysis did not affect the morphology of the MnO_2 nanowire. The presence of these camphoric carbon nano-beads on the MnO_2 nanowires have shown to increase the surface area by ~25 %. This porous composite electrode morphology showed advantages especially from points of higher energy and power density as compared to MnO_2 nanowire alone.

REFERENCES

1. K.R. Prasad, N. Munichandraiah, J. Power Sources 112 (2002) 443.
2. T.C. Girija, M.V. Sangaranarayanan, J. Power Sources 156 (2006) 705.
3. C. Arbizzani, M.C. Gallazzi, M. Mastragostino, M. Rossi, F. Soavi, Electrochem.Commun. 3 (2001) 16.
4. D. Belanger, X. Ren, J. Davey, F. Uribe, S. Gottesfeld, J. Electrochem. Soc.147 (2000) 2923.
5. A. Vinu, V. Murugesan, W. Bohlmann and M. Hartmann, J. Phys. Chem. B, 2004, 108, 11496.
6. S. C. Pang, M. A. Anderson and T. W. Chapman, J. Electrochem. Soc., 2000, 147, 444.
7. M. Mastragostino, C. Arbizzani and F. Soavi, J. Power Sources, 2001, 97, 812.
8. S. F. Chin, S. C. Pang and M. A. Anderson, Mater. Lett., 2010, 64, 2670.
9. Y. Sakamoto, M. Kaneda, O. Terasaki, D. Zhao, J. M. Kim, G. D. Stucky, H. J. Shin and R. Ryoo, Nature, 2000, 408, 449.
10. S. Alam, C. Anand, K. Ariga, T. Mori and A. Vinu, Angew. Chem., Int. Ed., 2009, 48, 7358.
11. A. Vinu, P. Srinivasu, M. Miyahara and K. Ariga, J. Phys. Chem. B, 2006, 110, 801.
12. A. Vinu, D. K. Sawant, K. Z. Hossain, K. Ariga, S. B. Halligudi and M. Hartmann, Chem. Mater., 2005, 17, 5339.
13. Y. I. Jang, B. Haung, F. C. Chou, R. D. Sadoway and Y. M. Chiang, J. Appl. Phys., 2000, 87, 7382.
14. S. C. Pang, M. A. Anderson and T. W. Chapman, J. Electrochem. Soc., 2000, 147, 444.
15. H. Xia, Y. Wang, J. Lin, L. Li, Nanoscale Res. Lett. 7 (2012) 33.

LIST OF PUBLICATIONS

1. Ultra fine MnO_2 nanowire based high performance thin film rechargeable electrodes†: Effect of surface morphology, electrolytes and concentrations (2012) Ranjusha R, A. S. Nair, S. Ramakrishna, Anjali P, Sujith K, K. R. V. Subramanian, Sivakumar N, T.N.

Kim, Shantikumar V Nair, A. Balakrishnan, *J. Mater. Chem.*, 2012, 22, 20465-20471.

2. Fabrication and performance evaluation of button cell supercapacitors based on MnO_2 nanowire/carbon nanobead electrodes† R Ranjusha, S Ramakrishna, S Nair, P Anjali, V Sukumaran, TS Sonia, A. Balakrishnan *RSC Adv.*, 2013,3, 17492-17499.
3. Supercapacitors based on freeze dried MnO2 embedded PEDOT: PSS hybrid sponges, Ranjusha R, Sajesh K. M, Roshny S, Lakshmi V, Anjali P, Sonia T. S., A. Sreekumaran Nair, K. R. V. Subramanian, Shantikumar V Nair, K P Chennazhi, A. Balakrishnan, *Microporous and Mesoporous Materials* 186 (2014) 30–36.

PATENT

1. The art, method, manner, process and system of fabricating uniform sized MnO_2 nanofibers. (*Indian patent 1866/CHE/2012*).
2. Method of fabricating highly porous thin film MnO_2 electrode for supercapacitors. (*Indian patent 1869/CHE/2012*).
3. The method, manner, process of nanocomposites of camphor derived carbons and metal oxide materials for high performance rechargeable electrodes for battery and supercapacitor applications. (*Indian patent 4449/CHE/2012 A*).